0270-9139/83/0306-0989$02.00/0
HEPATOLOGY

Vol. 3, No. 6, pp. 989–1001, 1983
Printed in U.S.A.

Mallory Body Formation Runs Parallel to γ-Glutamyl Transferase Induction in Hepatocytes of Griseofulvin-Fed Mice

JUNICHI TAZAWA, TETSUYA IRIE, AND SAMUEL W. FRENCH

Department of Pathology, Veterans Administration Medical Center, Martinez, California 94553 and University of California School of Medicine, Davis, California 95616

To evaluate whether Mallory bodies (MBs) are linked to the induction of the enzyme γ-glutamyl transferase (GGT), mice were fed 2.5% griseofulvin (GF). The experimental and control mice livers were examined at four time periods, i.e., after 4 months' of GF feeding, 1 month after GF withdrawal and 13 days after GF refeeding, and at sacrifice after 4 months of GF withdrawal. The livers from mice continuously fed GF or control diet for 10 months were also examined. Tumors and nontumorous livers were examined histologically, histochemically, electron microscopically, and immunocytochemically. The tumors consisted of hepatomas and hyperplastic nodules. To localize MBs inside GGT-positive cells, a double-staining method was employed; GGT-positive cells were identified histochemically followed by staining for MBs using the unlabeled immunoperoxidase technique. The per cent area of the GGT-positive foci was closely correlated with the frequency of MBs observed in the course of a GF feeding and withdrawal. Almost all of the MBs were located in GGT-positive cells in both tumors and nontumor liver tissue. MBs and GGT positivity involved the same liver cells. They both were found in high frequency in tumors induced by GF. These results indicate that MB formation, like GGT induction, is a phenotypic change induced by GF. The coexistence of the two phenomenon in the same cell throughout all phases of tumor formation suggests that MBs may be related to the neoplastic process in the GF-fed mouse model.

Since Mallory body (MB)-like filament formation is associated with neoplastic behavior in a tissue culture cell line derived from a rat hepatoma (1–6) and since MB formation is associated with toxic hepatitis an hepatoma in mice fed the carcinogens, griseofulvin (GF), or dieldrin (7–9), we postulated that Mallory bodies (MBs) are a putative marker for preneoplastic change (9–11). To test this hypothesis, we studied the association of MBs with the development of hepatocellular foci positive for γ-glutamyl transferase (GGT) activity, because GGT activity measured histochemically is considered to be a reliable marker of phenotypically altered hepatocytes in mice and rats during hepatoma induction (12–36). To study the coexistence of MBs and GGT induction in hepatocytes in the livers of mice fed GF during the development of GGT-positive foci, we also studied hyperplastic nodules and hepatomas.

MATERIALS AND METHODS

ANIMALS

Twenty-three male C3H mice (age 2 to 4 months) were fed *ad libitum* a protein-rich semisynthetic, complete standard Teklad Test Diet to which 2.5% GF was added. The experimental design is outlined in Figure 1. Fourteen control mice were fed the basic diet without GF added. The livers of 12 GF-fed (Group 1) and six control (Group 2) mice were biopsied three times surgically under methoxyfluorene anesthesia, i.e., after 4 months of GF feeding, 1 month after GF withdrawal, and 13 days after GF refeeding (Figure 1). Eleven mice were fed GF continuously for 10 months (Group 3), and eight mice were fed the control diet continuously for 10 months (Group 4) (Figure 1). Six mice of Group 1 and three of Group 2 died during or after the first and third operation, respec-

Received January 17, 1983; accepted June 20, 1983.
This work was supported by a Veterans Administration Research Support Grant.
This work was presented at the 33rd Annual Meeting of the American Association for the Study of Liver Diseases, Chicago, Illinois, November 2–3, 1982.
The work about preparation and characterization of anti-Mallory body antiserum was presented at the 66th FASEB Meeting, New Orleans, Louisiana, April 15–23, 1982 and published as an abstract (*Fed. Proc.* 1982; 44:392).
Address reprint requests to: Samuel W. French, M.D., Department of Pathology, School of Medicine, University of Ottawa, Ottawa, Ontario, Canada.

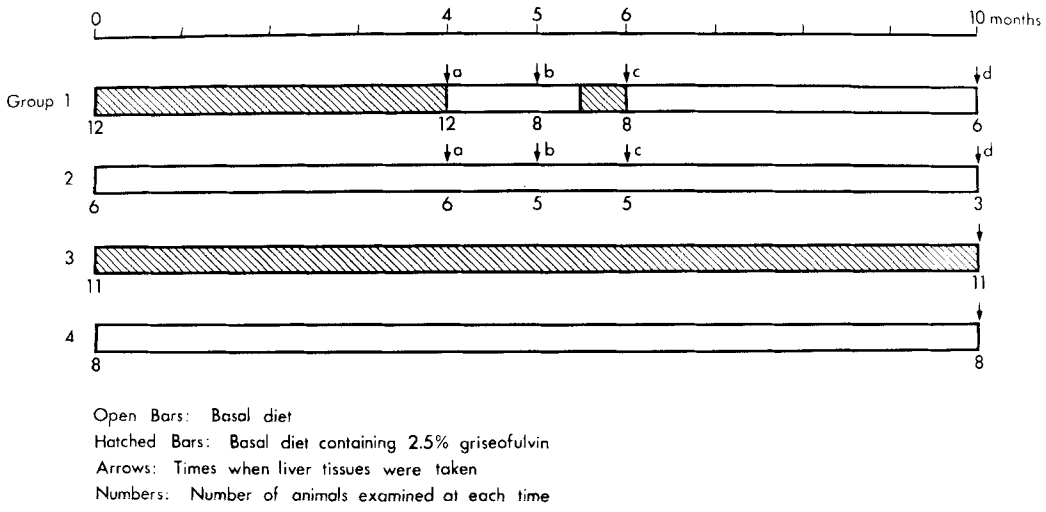

FIG. 1. Schematic representation of experimental design protocol.

tively, as shown in Figure 1. All mice were sacrificed at 10 months (Figure 1), and their livers were cut into 2-mm-thick slices to collect tumors and nontumor liver tissue for processing. Three of the 11 livers from mice fed GF for 10 months (Group 3) were examined to include nontumor liver tissue but only tumors present on the surface were processed. Tumors measuring over 2 mm in size were collected. Tumors consisted of hyperplastic nodules and hepatomas. Hepatomas were diagnosed when diagnostic trabecular pattern was observed. The remaining liver which included foci or nodules measuring up to 2 mm was defined as nontumor liver tissue.

HISTOCHEMISTRY

Portions of the tumors were fixed in formalin and embedded in paraffin for light microscopic observation by hematoxylin and eosin staining. Separate blocks of nontumor liver tissue and tumors were frozen quickly in liquid nitrogen, and sections were cut 6-μm thick using a cryostat. The tissue sections were cold acetone fixed 2½ hr and air dried for histochemical enzyme assay for GGT (37). Each tissue assay was done in duplicate. Controls for GGT histochemistry included a no substrate control, a boiled control, and a positive kidney control. Serial sections were stained with hematoxylin and eosin after 2 min of methanol fixation for counting MBs. Sections stained for GGT activity were projected onto paper mounted on the wall at a standard distance and magnification by using a projecting lens (Proj.-Ok.H 3.2 ×, Ernest Leitz Wetzlar, Germany), and GGT-positive foci were sketched on the paper. A GGT-positive focus was defined as an area in more than two adjacent canaliculi stained for GGT activity or the cell cortex of at least one hepatocyte stained for GGT activity. Bile duct staining normally observed in both experimental and control livers was excluded on the basis of the characteristic branching and architecture. Foci measuring up to 2 mm in size, and nodules and hepatomas were assessed for GGT activity and MB content.

IMMUNOCYTOCHEMISTRY

A double-staining method for GGT activity and MBs was employed to localize MBs inside GGT-positive cells. Nontumor liver tissue from GF-refed mice (Group 1c), GF withdrawn mice (Group 1d), and 10 months GF-fed mice (Group 3) and control mouse livers (Groups 2c, 2d, and 4), and tumors were studied in this way. First, the tissue was stained for GGT activity histochemically, then the tissue sections were incubated in 0.5% H_2O_2 in 0.05 *M* EDTA in phosphate-buffered saline (pH 7.2) (PBS-EDTA solution) to block endogeneous peroxidase for 30 min at room temperature. After rinsing in PBS-EDTA solution, 3% goat whole serum was applied as a blocking antibody for 30 min at room temperature. Rabbit anti-MB antibody (1:500 dilution in 1% goat whole serum) was applied, and sections were incubated overnight at 4°C. After rinsing in PBS-EDTA solution, goat anti-rabbit IgG (1:10 dilution) was applied for 30 min at room temperature. After rinsing in PBS-EDTA solution, rabbit peroxidase antiperoxidase complex in 1% goat whole serum (1:50 dilution) was applied for 30 min at room temperature. After rinsing in PBS-EDTA solution, 0.04% 4-chloro-1-naphthol (blue color) in 0.05 *M* Tris buffer (pH 7.60) with 0.001% H_2O_2 was used for color development to avoid confusion with protoporphyrin pigment (brown color) in nontumor liver tissue of GF-fed mice. This substrate solution was applied for 30 min at 37°C. 4-chloro-1-naphthol solution was prepared using a modification of the procedure described by Nakane (38): 40 mg of 4-chloro-1-naphthol with 6.055 gm Trizma base was stirred overnight to dissolve it in 70 ml of distilled water followed by pH adjusted to 7.60 using 2*N* HCl and finally brought to 100 ml with distilled water. After rinsing in distilled water, sections were mounted with water-soluble mounting medium. The chromogen 3-3'-diaminobenzidine (DAB) in 0.05 *M* Tris buffer (pH 7.6) was used for the color development in tumors and control mouse liver. DAB was used in tumors and control liver because these tissues were free of protoporphyrin pigment. The brown product formed with DAB is easier to visualize than the blue product formed from naphthol. Goat whole serum, goat anti-rabbit IgG, and rabbit peroxidase antiperoxidase complex were purchased from Cappel Laboratories, (Cochranville, Pa.). Control stains were run in parallel in all cases using preimmune rabbit serum to rule out nonspecific staining.

Preparation and Characterization of Anti-MB Antiserum

MBs were isolated from a human autopsied liver using a modification of French's method (39). Purity was assessed by electron microscopic examination of the pellet. Polypeptide bands of MB protein were prepared by sodium dodecyl sulfate polyacrylamide (10%) gel electrophoresis (40). Antiserum against the major 45K polypeptide derived from the MB was raised in a rabbit using bands excised from polyacrylamide gels (41). Gel strips containing approximately 200 μg of protein were homogenized in 1 ml of 0.01 *M* PBS (pH 7.0), emulsified with the same volume of complete Freund's adjuvant, and injected by multiple site subcutaneous injections. Six booster injections were followed at 2-week intervals in the same manner except incomplete Freund's adjuvant was used. The animal was bled at 2-week intervals over 8 months after the first booster injection. Antibody production was monitored immunocytochemically by the indirect peroxidase-antiperoxidase method using formalin-fixed, paraffin-embedded, and trypsin-digested human liver biopsy samples of alcoholic hepatitis (42, 43). The antiserum stained MBs up to a dilution of 1:10,000. The optimal titer for staining MBs was determined to be 1:500 dilution. Characterization of the antiserum was done using immunocytochemically and immunoelectron microscopy techniques. The antiserum was repeatedly absorbed with freshly isolated human MBs. Affinity purified anti-MB antibody was obtained by eluting antibody from MBs which were used for absorption (44). The antibody was eluted with glycine-HCl buffer (pH 2.7), dialyzed against PBS (pH 7.2), and stored at −20°C. The anti-MB antiserum and affinity purified anti-MB antibody stained MBs, the cytoplasm and cell cortex of hepatocytes, and bile duct epithelial cells. The results were the same as reported by Kimoff and Huang (45). These structures did not stain with preimmune serum or absorbed anti-MB antiserum. Immunoelectron microscopy using Triton × 100 extracted liver from GF-fed mice (46) showed that the MB filaments selectively stained with antibody as indicated by the finding that each MB filament was coated with reaction product.

Immunoelectron Microscopy

Sections double stained for GGT and MBs by using DAB as substrate were dehydrated in ethanol, mounted in Permount, and checked by light microscopy. After removal of the cover slips by immersion in xylene, the sections were rehydrated in ethanol, rinsed in 0.1 *M* sodium cacodylate buffer (pH 7.4), and fixed in 1% osmium tetroxide for 1 hr. After rinsing with sodium cacodylate buffer, the sections were dehydrated in ethanol and processed by using Bretschneider's pop-off technique (47). Thin sections were observed using a Zeiss 109R electron microscope.

Electron Microscopy

The specimens were fixed in ice-cold 2.5% glutaladehyde in 0.1 *M* sodium cacodylate buffer (pH 7.4). After washing in sodium cacodylate buffer, the tissue was postfixed in 1% osmium tetroxide in sodium cacodylate buffer for 1 hr. After rinsing in sodium cacodylate buffer, the tissue was *en bloc* stained with 2% uranyl acetate in 15% ethanol, dehydrated in graded ethanol, and embedded in Spurr's resin. One-micron sections were stained with toluidine blue, and representative blocks were thin-sectioned and stained with uranyl acetate and lead citrate, and observed using a Zeiss 109R electron microscope.

Morphometry

In nontumor liver tissue, both the number and the area of the GGT-positive foci were measured morphometrically by a computerized instrument (Videoplan, Zeiss). In tumors, the area of GGT-positive cells was measured in the same way. The number of foci was expressed as number per square millimeter area. The area of the GGT-positive foci was expressed as a percentage of GGT-positive foci area in square millimeter

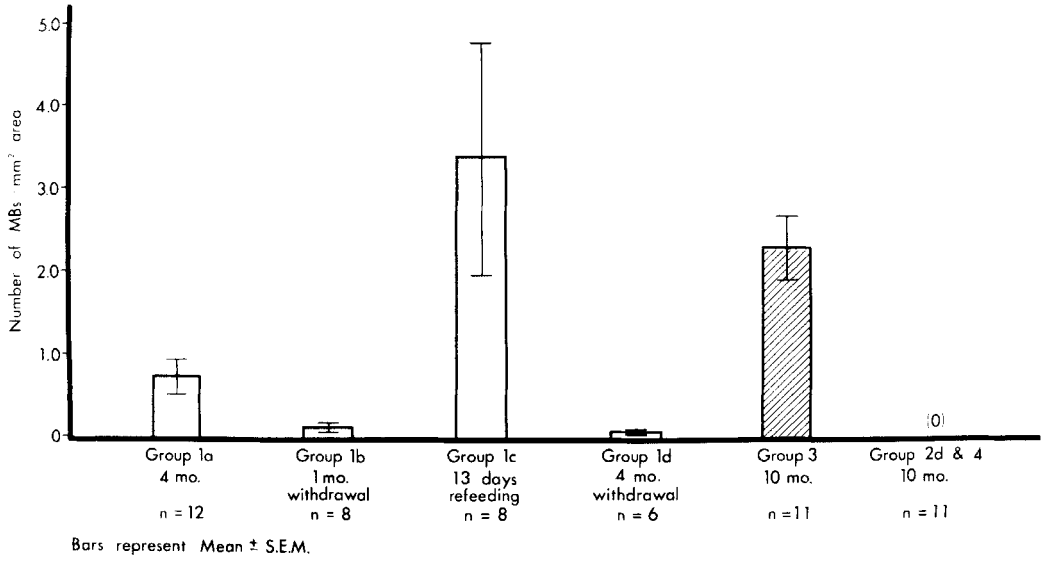

FIG. 2. Frequency of MBs found in hematoxylin and eosin sections of nontumor liver tissue from GF-fed and control mice.

per total area in mm^2. The number of MBs in both the GGT-positive area and the GGT-negative area observed by light microscopy were counted. The number of MBs was expressed as number per square millimeter.

STATISTICS

The data obtained were analyzed using the Student's t test. Mann-Whitney U-test was employed instead of Student's t test when the data consisted of many zeros which prevented normal distribution (indicated by "z" after p values). Values were expressed as mean ± S.E.

RESULTS

HISTOPATHOLOGY

Nontumor Liver Tissue. Liver tissue free of tumors measuring over 2 mm were analyzed for the presence of MBs. MBs (number per square millimeter area) were found in all but one GF-fed mouse liver in sections

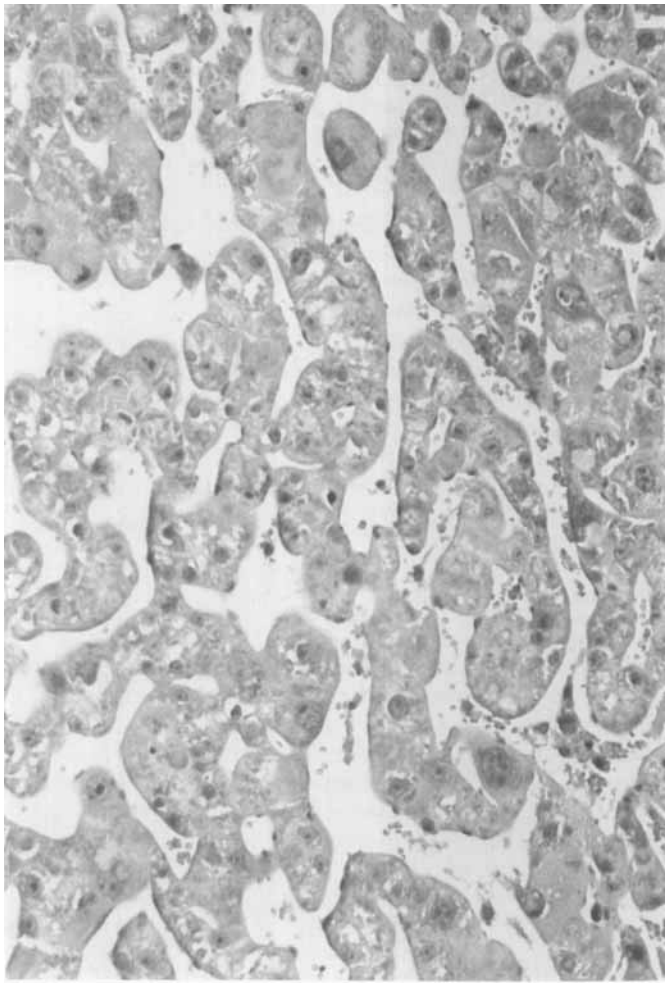

FIG. 3. A hepatoma from a mouse fed GF for 10 months showing a typical diagnostic trabecular pattern. H & E, × 122.

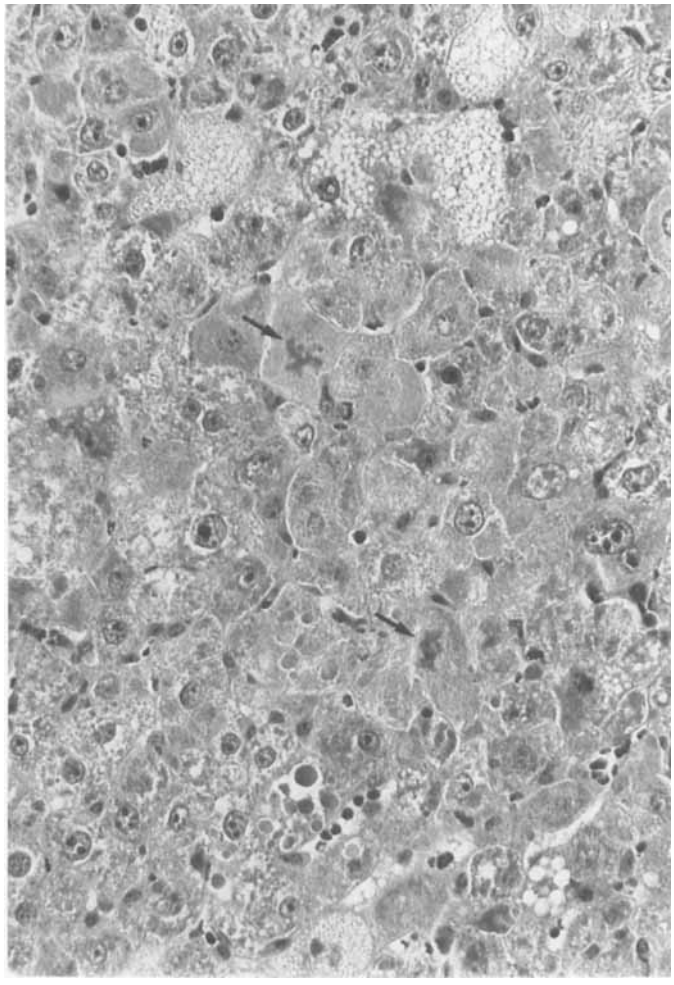

FIG. 4. A hyperplastic nodule from a mouse fed GF for 10 months showing a variety of cell patterns. Some hepatocytes demonstrate MBs (*arrows*). H & E, × 190.

TABLE 1. NUMBER AND SIZE OF TUMORS

Group	Treatment	No. of mice	Mice-bearing tumor		Tumor	No. of tumors	Average no. of tumors per liver	Average size of tumors[a] (mm)
			No.	%				
1d	GF withdrawal	6	3	50%	Hyperplastic nodule	4	1.3 ± 0.3	3.1 ± 0.7[b]
2d & 4	Control	11	3	27	Hyperplastic nodule	8	2.7 ± 0.3	5.5 ± 1.2
3	GF continuous	11	11	100	Hyperplastic nodule	69	8.3 ± 0.9[d]	4.7 ± 0.2[c]
3	GF continuous		5	46	Hepatoma	7		6.9 ± 0.8

Results are expressed as mean ± S.E.

[a] Tumor size is expressed as the mean of (long axis + short axis).

[b] $p < 0.01$ when Group 1d is compared with Group 3 hepatoma.

[c] $p < 0.01$ when Group 3 hyperplastic nodule is compared with Group 3 hepatoma.

[d] Only completely analyzed livers are included (n = 8).

All other comparisons were not statistically significant.

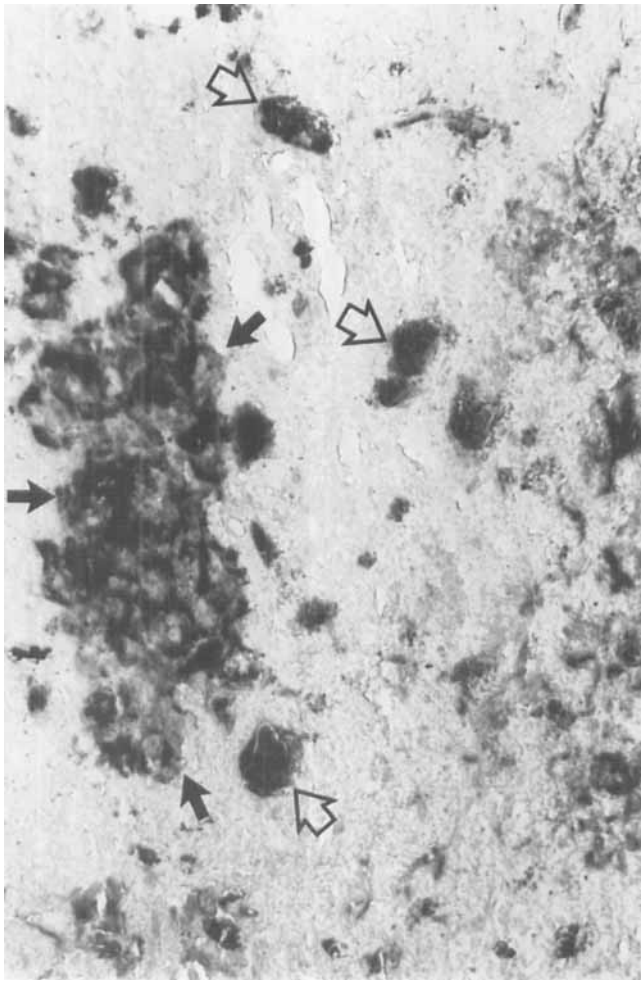

FIG. 5. Nontumor liver tissue from a GF-refed mouse (Group 1c) showing a discrete focus of GGT-positive hepatocytes (*solid arrows*). Protoporphyrin pigment (*open arrows*) is present scattered in the lobule. GGT, × 122.

stained with hematoxylin and eosin at 4 months of GF feeding (0.72 ± 0.20, mean ± S.E.). MBs were decreased after GF withdrawal (0.11 ± 0.06, $p < 0.01^z$) and were increased again after GF refeeding (3.33 ± 1.38, $p < 0.02^z$), and were decreased again after 4 months of GF withdrawal (0.08 ± 0.05, $p < 0.01^z$) (Figure 2). The frequency of MBs found in the livers of mice fed GF for 10 months (Group 3) was 2.28 ± 0.38. This was not significantly different from that of GF-refed mice (Group 1c). No MBs were found in control livers (Groups 2a, 2b, 2c, 2d, and 4) (Figure 2).

Tumor. Eighty-eight tumors more than 2 mm in size were identified from all groups at 10 months. The number of hyperplastic foci under 2 mm was not quantitated. In mice fed GF for 10 months, seven hepatomas showing diagnostic trabecular pattern were found (Figure 3). They were larger (6.9 ± 0.8 mm) than 69 hyperplastic nodules from mice fed GF for 10 months (4.7 ± 0.2, $p < 0.01$) and four hyperplastic nodules from GF withdrawn mice (3.1 ± 0.7, $p < 0.01$) (Table 1). MBs were found in tumors including hepatomas in sections stained with hematoxylin and eosin but this method was not as sensitive a method for detecting MBs as was immunocytochemistry. In one hepatoma, many MBs were found to be surrounded by neutrophils. Hyperplastic nodules from GF-fed mice showed various cell types, i.e., eosinophilic cells, basophilic cells, foamy cells, fat-bearing cells, and MB-bearing cells (Figure 4). Spontaneous hyperplastic nodules from controls showed no MB-bearing cells.

HISTOCHEMISTRY

Nontumor Liver Tissue. GGT-positive foci of liver cells were found in all livers of GF-fed mice. Bile duct staining was observed in all livers examined. The lobular distribution of the GGT-positive foci was not studied. GGT activity was generally detected in the canalicular region (Figure 5). Sometimes it was also found at the cell border. Slight staining of the cytoplasm was sometimes present

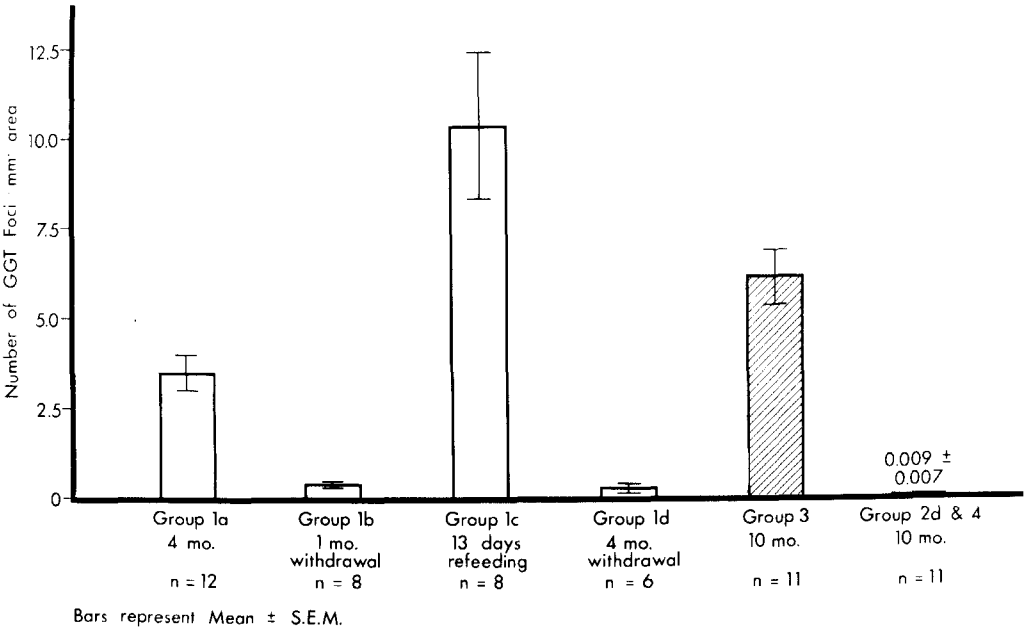

FIG. 6. Frequency of GGT-positive foci in the nontumor liver tissue from GF-fed and control mice.

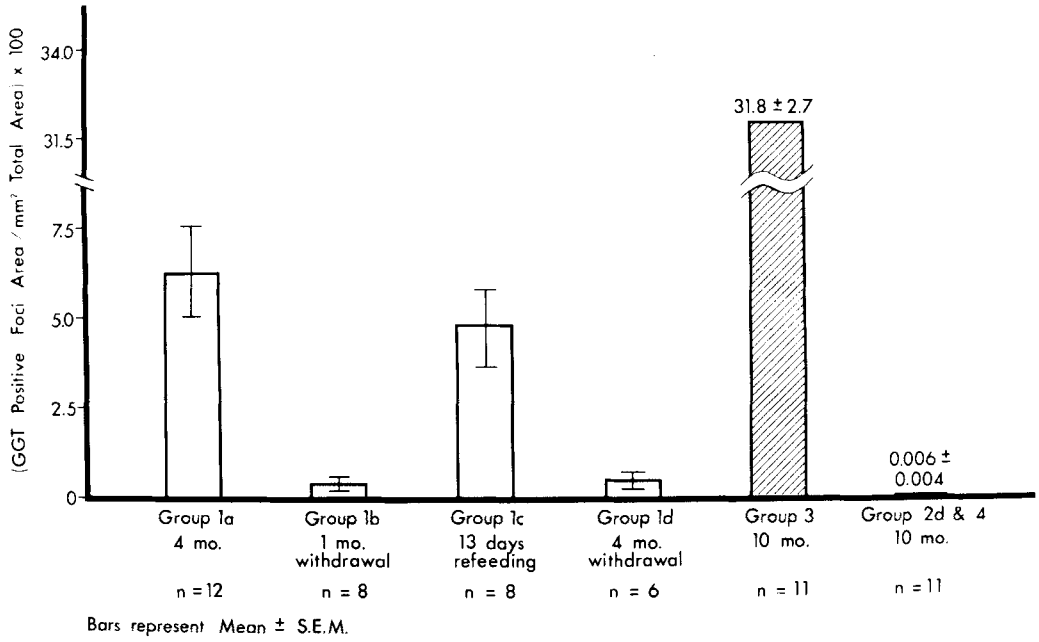

FIG. 7. GGT-positive foci area expressed as a percentage of total area in the nontumor liver tissue from GF-fed and control mice.

mainly after 10 months of GF feeding (Group 3). The number of GGT-positive foci per mm^2 area was 3.55 ± 0.56 at 4 months of GF feeding. This number decreased after GF withdrawal (0.40 ± 0.04, $p < 0.001$), increased again after GF refeeding (10.23 ± 2.00, $p < 0.001$), and decreased again after 4 months of GF withdrawal (0.23 ± 0.13, $p < 0.001$) (Figure 6).

The changes in the frequency of GGT-positive foci during the course of GF feeding and withdrawal were closely correlated with changes in the frequency of MBs as shown in Figure 2. The number of GGT-positive foci per mm^2 area in the livers of mice fed GF for 10 months (Group 3) was 6.09 ± 0.75. This number was smaller than that in GF-refed mice (Group 1c) ($p < 0.05$). Only bile ducts and a single canaliculus were positive for GGT in the control livers until 6 months (Groups 2a, 2b, and 2c). No GGT-positive foci were observed in these control livers. Only one GGT-positive hepatocyte was found in 2 of 11 control livers at 10 months (Groups 2d and 4), where the GGT reaction was limited to the cell cortex (Figure 6).

The per cent GGT-positive foci area per total area was 6.23 ± 1.28 at 4 months of GF feeding. The per cent GGT-positive foci decreased after GF withdrawal (0.39 ± 0.16, $p < 0.005$), increased again after GF refeeding (4.68 ± 1.19, $p < 0.005$), and decreased again after 4 months of GF withdrawal (0.42 ± 0.16, $p < 0.02$) (Figure 7).

The changes in the per cent of GGT-positive foci area during the course of GF feeding and withdrawal were closely correlated with changes in the frequency of MBs as shown in Figure 2. The per cent GGT-positive foci area per total area in the livers of mice fed GF continuously for 10 months (Group 3) was 31.8 ± 2.7 which is higher than that in GF-refed mice (Group 1c) ($p < 0.001$) (Figure 7).

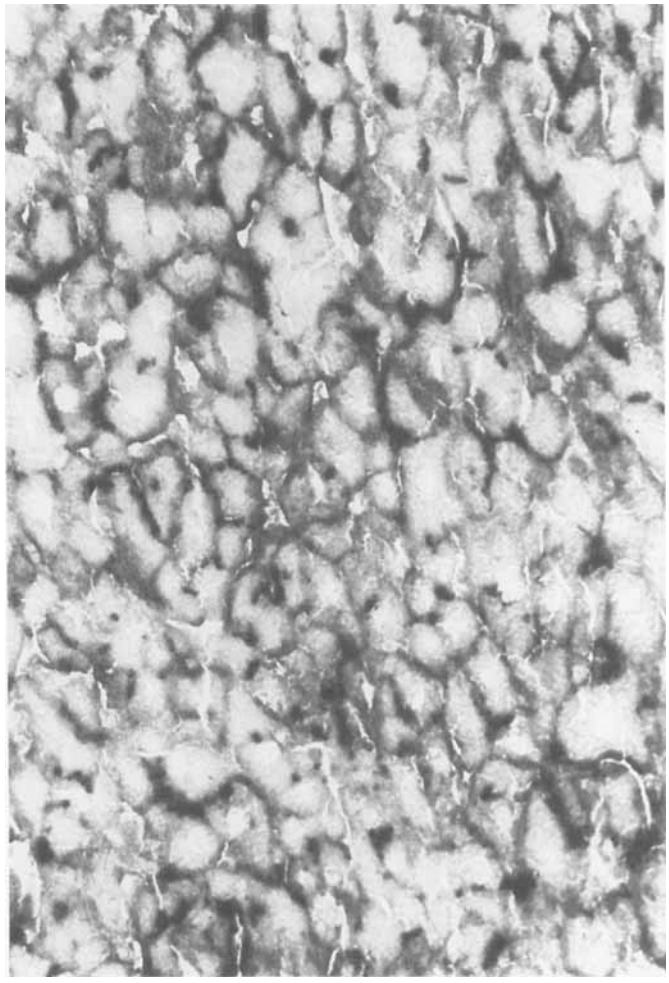

FIG. 8. A hepatoma from a mouse fed GF for 10 months showing intense GGT activity localized at the cell borders and canaliculi. GGT, × 190.

Tumor. Seventy-two of 73 (99%) hyperplastic nodules and all of seven hepatomas from GF-fed mice showed GGT activity (Table 3). GGT activity was frequently detected at the cell borders in hyperplastic nodules and hepatomas (Figure 8). Both canalicular and cytoplasmic activities were noted (Figure 9). The per cent GGT-positive area per total area of 69 hyperplastic nodules and seven hepatomas from mice fed GF continuously for 10 months were 76.8 ± 3.5 and 74.8 ± 10.8%, respectively.

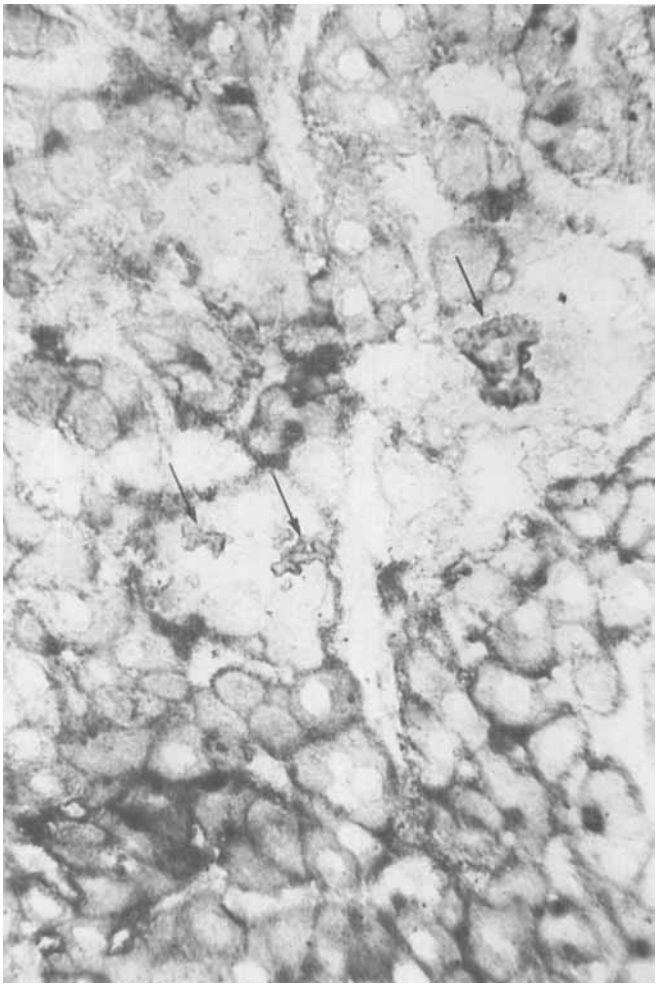

FIG. 9. A hepatoma from a mouse fed GF for 10 months showing MBs (*arrows*) within neoplastic hepatocytes. GGT activity is localized at the cell borders. Both canalicular and cytoplasmic activities are also noted. When viewed in color, the MBs stain blue and the GGT reaction product stains orange-red so the two are easily distinguished. Double-staining method, × 144.

This is more than double that of the nontumor tissue at 10 months of continuous feeding (Group 3, 31.8 ± 2.7%) and 15 times that of the 13-day GF refed mice (Group 1c). One of 8 spontaneous tumors (Groups 2d and 4) showed focal GGT-positive cells in control mice (Tables 2 and 3).

It should be emphasized here that the GGT-positive foci data was obtained using two-dimensional measurements. Since this data does not correct for the size and shape of the foci, it does not accurately reflect the three-dimensional volumes of the foci (48).

IMMUNOCYTOCHEMISTRY

Nontumor Liver Tissue. Double staining for GGT and MBs revealed MBs which stained blue within orange-stained GGT-positive foci. It was easy to distinguish MBs from protoporphyrin pigment because of the blue reaction when 4-chloro-1-naphthol was used as substrate. Almost all of the MBs were detected within GGT-positive foci (Figure 10). The preimmune serum controls showed only GGT-positive foci without staining of MBs (Figure 11). The per cent GGT-positive foci area per total area and the number of MBs per mm^2 total area based on the double-staining method in the nontumor liver tissue from GF-refed mice (Group 1c) were closely correlated ($r = 0.8362$, $p < 0.01$) (Figure 12). The same was true for mice fed griseofulvin continuously for 10 months ($r = 06213$, $p < 0.05$).

Tumor. The double-staining method revealed many MBs, mainly within GGT-positive neoplastic cells in both hyperplastic nodules (Figure 14) and hepatomas (Figure 9). No MBs were seen in spontaneous tumors (Table 3). Both GGT and MBs were found in high frequency in hepatomas from mice fed GF continuously for 10 months (100 and 71%, respectively) and hyperplastic nodules from GF-fed mice (99 and 86%, respectively) (Table 3). It is noteworthy that a few GGT-positive foci with MBs remained in 2 of 4 hyperplastic nodules and 5 of 6 livers (tumor-free liver tissue) after 4 months of GF withdrawal (Group 1d), suggesting this change was partially reversible (Figure 10, Tables 2 and 3). The number of MBs per mm^2 GGT-positive area was significantly higher than the number of MBs per mm^2-negative area in nontumor liver tissue at 13 days after GF refeeding, after 4 months of GF withdrawal, after 10 months of continuous GF feeding, and in hyperplastic nodules from mice fed GF continuously for 10 months (Table 4). This verifies the observation that almost all of the MBs were located within GGT-positive cells. As

TABLE 2. PATTERN OF GGT AND MBS IN THE TUMORS BASED ON THE DOUBLE-STAINING METHOD

Group	Treatment	No. of mice	Tumor	GGT and MB patterns				Total
				GGT(+) MB(+)	GGT(+) MB(−)	GGT(−) MB(+)	GGT(−) MB(−)	
1d	GF withdrawal	6	Hyperplastic nodule	2[a]	1	0	1	4
2d & 4	Control	11	Hyperplastic nodule	0	1	0	7	8
3	GF continuous	11	Hyperplastic nodule	61	8	0	0	69
3	GF continuous	5	Hepatoma	5	2	0	0	7

[a] Number of tumors showing each combination of the two markers

shown in Figure 15, a majority of MBs were localized within GGT-positive cells in both tumors and nontumor liver tissue. The number of MBs per mm^2 total area in MB-positive tumors (16.9 ± 4.4) was greater than that in the corresponding nontumor liver tissue (5.2 ± 1.1, $p < 0.02$), indicating MBs are more concentrated in tumors compared to nontumor liver tissue. However, the number of MBs per GGT-positive area in MB-positive tumors was not statistically different from that in corresponding GGT-positive foci in the nontumor liver tissue even though the trend was for an increase (Table 5). This was thought to be explained by the difference in per cent GGT-positive area per total area compared to the difference in the number of MBs per total area (Table 5). Thus, the per cent GGT-positive area of tumors did not correlate with the number of MBs per mm^2 of total tumor area (Figure 13).

TABLE 3. FREQUENCY OF GGT AND MBS IN THE TUMOR AND NONTUMOR LIVER TISSUE AT 10 MONTHS BASED ON THE DOUBLE-STAINING METHOD

Tissue	Group	No. of specimens	GGT positive		MB positive	
			No.	%	No.	%
Tumor						
Hepatoma	3	7	7	100	5	71
Hyperplastic nodule	1d & 3	73	72	99	63	86
Spontaneous tumor	2d & 4	8	1	13	0	0
Nontumor liver tissue						
4 mos. GF withdrawal	1d	6	5	83	5	83
10 mos. GF continuous	3	11	11	100	11	100
Control	2d & 4	11	2	18	0	0

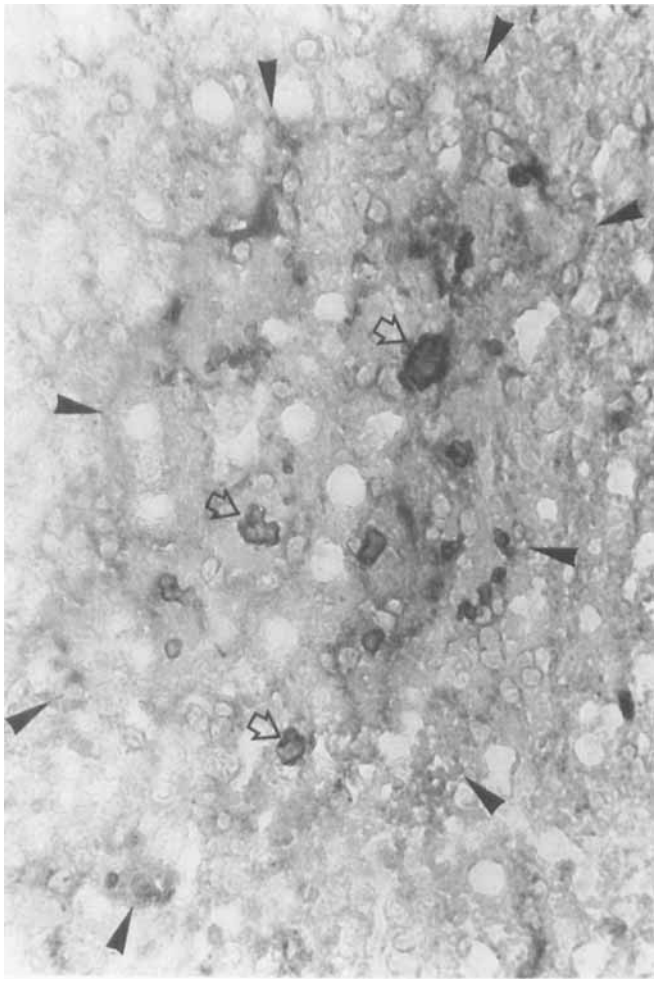

FIG. 10. Nontumor liver tissue from a mouse withdrawn from GF for 4 months (Group 1d) showing a GGT-positive focus (*solid arrows*) with MBs (*open arrows*). The enzyme staining of the bile canaliculi was obvious when viewed in color but is less striking as seen here in black and white. Double-staining method, × 285.

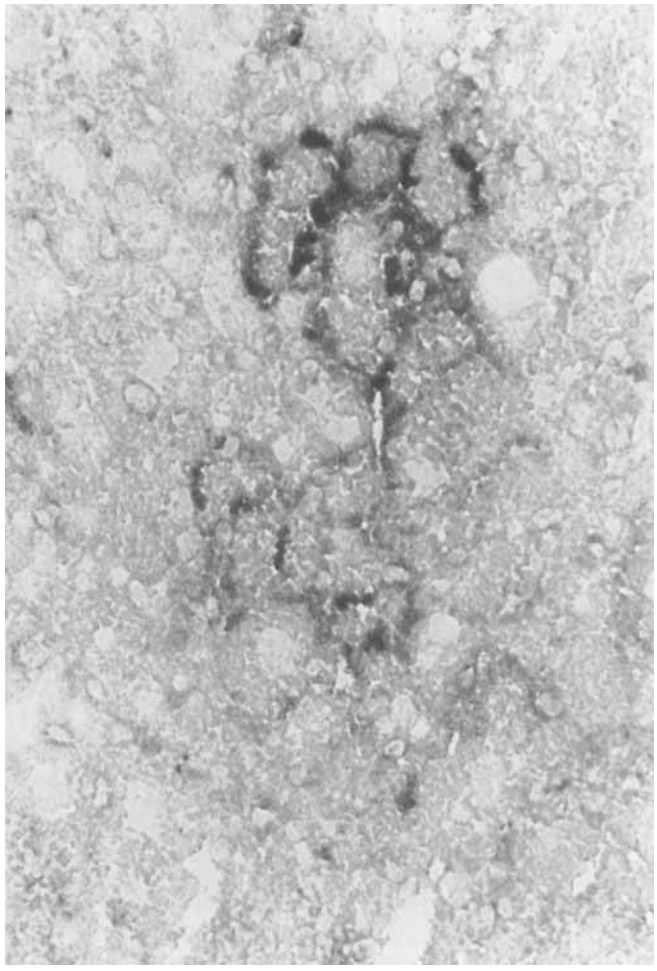

FIG. 11. Preimmune serum control of nontumor liver tissue from a mouse withdrawn from GF for 4 months (Group 1d). A GGT-positive focus is present but MBs are not stained with the control sera. Double-staining method, × 375.

IMMUNOELECTRON MICROSCOPY AND ELECTRON MICROSCOPY

Immunoelectron microscopy showed reaction product located at the margin of MBs (Figure 16). This correlated well with the light microscopic observations where reaction product was localized to the periphery of the MBs (Figures 9, 10, and 14). The presence of MBs was confirmed by conventional electron microscopy.

Electron microscopy of selected blocks of liver tissue revealed some characteristics of the hepatocytes in hyperplastic nodules, i.e., proliferation of smooth endoplasmic reticulum, decrease in glycogen and rough en-

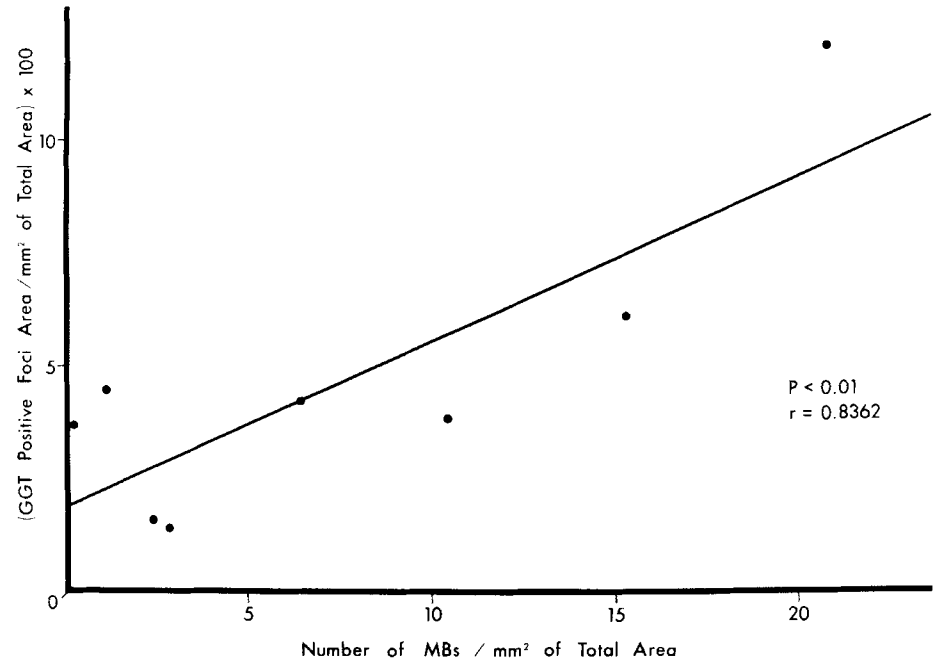

FIG. 12. GGT-positive foci area expressed as percentage of total area and the number of MBs per mm^2 of total area are correlated using nontumor liver tissue. The data are from eight mice refed GF for 13 days (Group 1c).

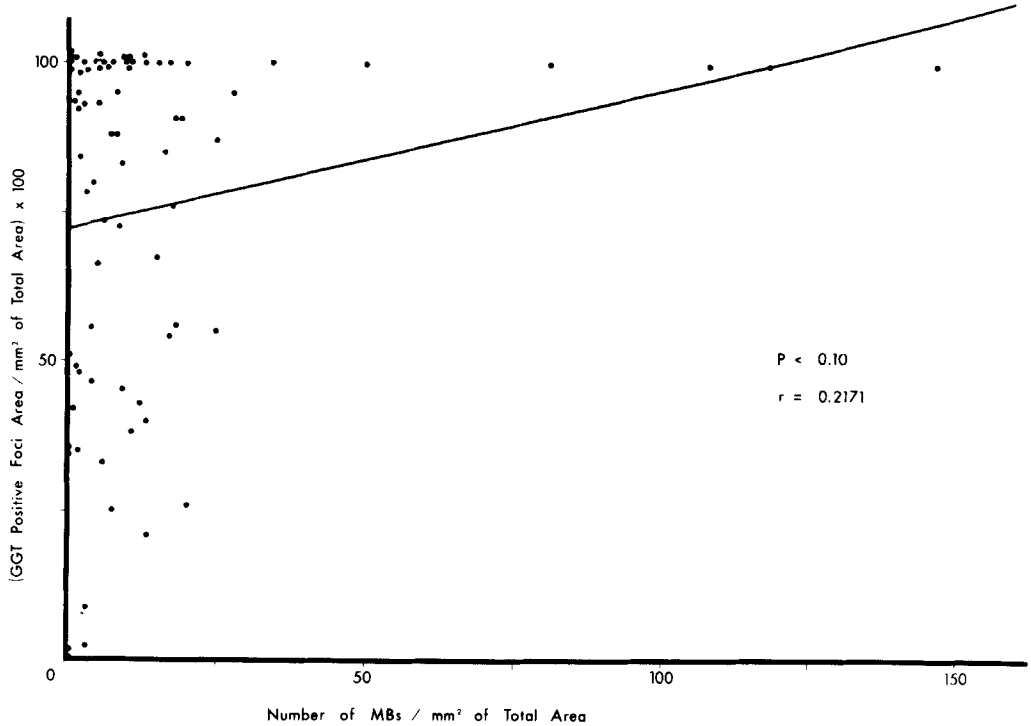

FIG. 13. GGT-positive foci area expressed as percentage of total area and the number of MBs per mm^2 of total area are correlated using liver tumor tissue from mice fed GF for 10 months. The data are from 7 hepatomas and 69 hyperplastic nodules.

doplasmic reticulum. In some areas, the loss of ectoplasm, microvilli, and canaliculi was observed. Examination of a hepatoma showed prominent canaliculi formation, prominent smooth and rough endoplasmic reticulum, and a focal increase in intermediate filaments. Details of our electron microscopic findings will be reported elsewhere.

DISCUSSION

By using a sensitive double-staining method for locating MBs within GGT-positive cells, a close relationship was observed between GGT positivity and the presence of MBs. That is, the frequency of GGT-positive foci (Figure 6) and the GGT-positive foci area expressed as

the percentage of total area (Figure 7) were closely correlated with the frequency of MBs in the course of GF feeding and withdrawal. Almost all of the MBs were located in GGT-positive cells in nonneoplastic livers and liver tumors. This finding suggests that MB formation, like GGT induction (12–36), is a phenotypic change that is somehow related to the neoplastic process. This conclusion is supported by two other observations. First, MBs occurred in high frequency and were more concentrated in tumors including hepatomas than in the corresponding nonneoplastic liver tissue. Second, MBs persisted after 4 months of GF withdrawal in both tumors and nontumor liver tissue indicating an autonomous process.

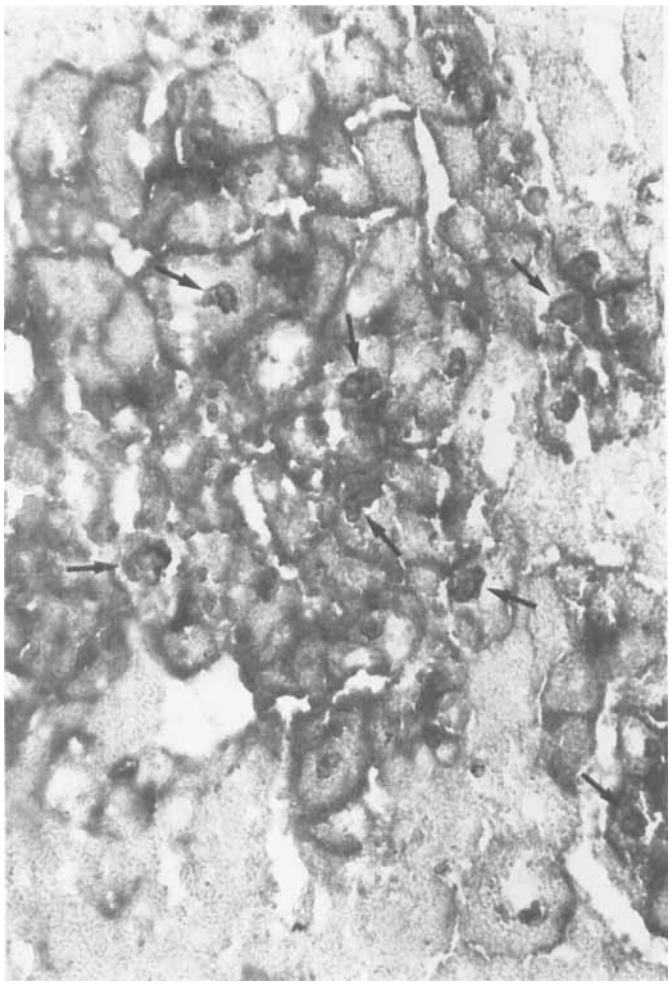

FIG. 14. A hyperplastic nodule from a mouse fed GF for 10 months showing MBs (*arrows*) within GGT-positive neoplastic cells. GGT activity is localized at the cell borders. Double-staining method, × 190.

There are two alternative hypotheses regarding the pathogenesis of MBs. However, neither of these, i.e., the microtubular failure hypothesis (49, 50) nor the vitamin A deficiency hypothesis (50), explains the persistence of MBs after 4 months of GF withdrawal.

Eight spontaneous tumors were found in 3 of 11 control mice (27%) and GGT activity was found in only one of these tumors. These findings are in agreement with other investigators' observations (24, 51). The reason why carcinogen-induced tumors develop GGT positivity and MBs and spontaneous tumors do not, needs to be clarified.

Goldfarb et al. (52) examined hyperplastic nodules for GGT activity in mice fed GF for 10 to 11 months followed by 2 to 6 months of withdrawal. GGT activity was found after the withdrawal of GF but positive staining was weak and focal. In contrast, our studies showed that a high percentage of GGT positive area per total area (76.8%) was found in hyperplastic nodules at 10 months of continuous GF feeding. This discrepancy may be explained by the effect of griseofulvin as an inducer and/or by remodeling GGT-positive foci and nodules after carcinogen withdrawal as was shown by Enomoto et al. (32). This fact may explain the very high percentage (31.8%) of GGT-positive foci area per total area of nontumor liver tissue observed at 10 months of GF feeding compared to the percentage at 4 months of GF feeding, and 13 days of GF refeeding (6.2 and 4.7%, respectively). Thus, there was a progressive increase in GGT-positive cells with time and with hyperplastic nodule formation as long as GF was fed. It should be pointed out here that the GGT-positive foci data was obtaied using two-dimensional measurements. Since this data does not correct for the size and shape of the foci in three dimensions, it does not accurately reflect the volumes of the foci (48).

In both hepatomas and hyperplastic nodules, GGT activity was frequently detected at the cell border and within the cytoplasm as well as around the canaliculi.

TABLE 4. LOCALIZATION OF MBS IN GGT POSITIVE FOCI COMPARED WITH GGT NEGATIVE AREA BASED ON THE DOUBLE-STAINING METHOD

Group	No. of mice	No. of MBs/mm² of GGT-positive area	No. of MBs/mm² of GGT-negative area	No. of MBs/mm² total area
Nontumor liver tissue				
13 days GF refeeding (Group 1c)	7	167.4 ± 42.6[a]	0.77 ± 0.22[a]	8.4 ± 2.8
4 mos. GF withdrawal (Group 1d)	5	134.9 ± 88.8[b]	0.032 ± 0.021[b]	0.5 ± 0.3
10 mos. GF continuous (Group 3)	11	14.3 ± 2.7[c]	0.38 ± 0.14[c]	5.2 ± 1.1
Tumors[e]				
37 hyperplastic nodules (Group 3)	10	19.4 ± 4.3[d]	2.2 ± 0.5[d]	9.5 ± 1.3

Results are expressed as mean ± S.E.: [a] $p < 0.005$; [b] $p < 0.01$ (Mann-Whitney U test was used in this analysis instead of Student's t test); [c,d] $p < 0.001$.

[e] Only tumors showing MBs and both GGT-positive and negative areas are included.

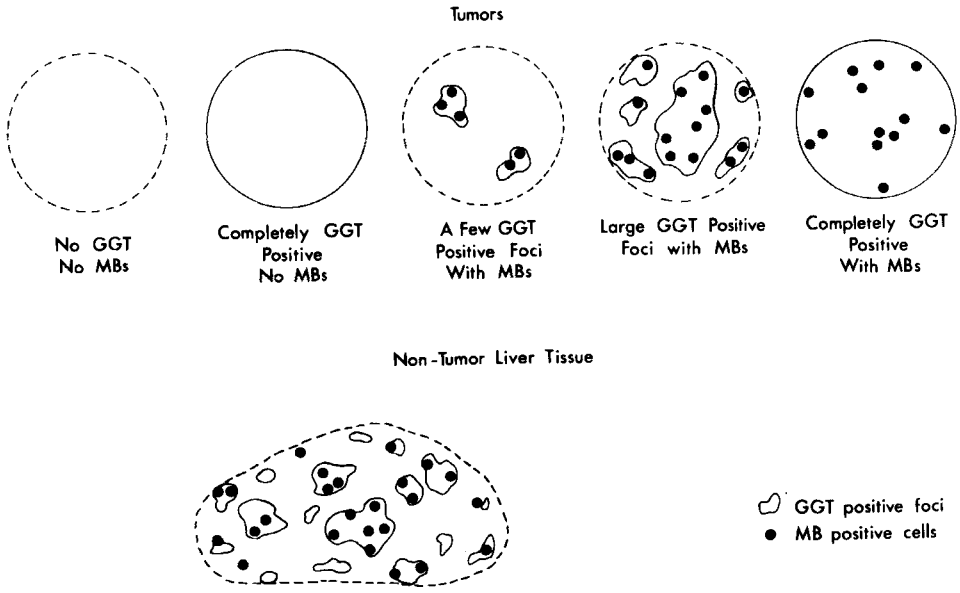

FIG. 15. Schematic drawing of types of tissue analyzed and the pattern of staining using a double-staining method for GGT and MBs. The majority of MBs were found in GGT-positive foci or neoplastic cells.

TABLE 5. COMPARISON OF THE FREQUENCY OF MBS FOUND IN MB-POSITIVE TUMOR AND NONTUMOR LIVER TISSUE FROM 11 CONTINUOUSLY GF-FED MICE

Tissue examined	No.	No. of MBs/mm² of total area	No. of MBs/mm² of GGT (+) area	GGT(+) area / Total area (%)
MB-positive tumors	66	16.9 ± 4.4[a,b]	22.2 ± 4.4	78.2 ± 3.4[c]
Nontumor liver tissue	11	5.2 ± 1.1	14.3 ± 2.7	31.8 ± 2.7

[a] Mean ± S.E.
[b] $p < 0.02$ when MB-positive tumors are compared with nontumor liver tissue.
[c] $p < 0.001$ when MB-positive tumors are compared with nontumor liver tissue.

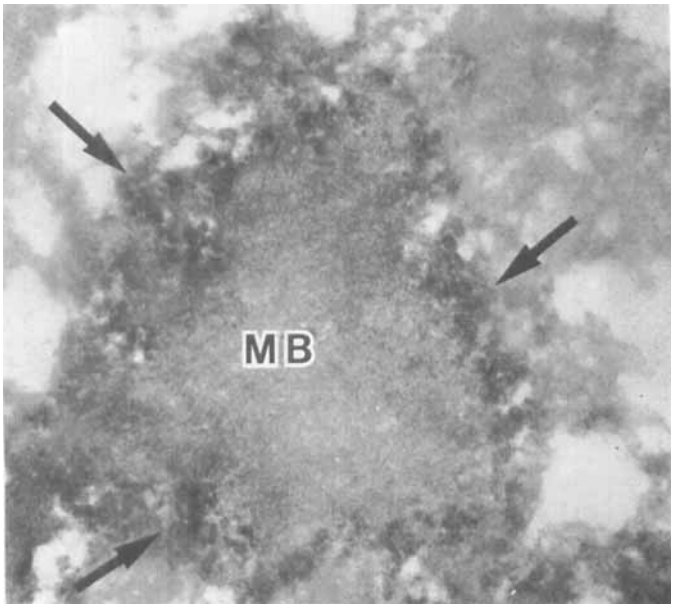

FIG. 16. An immunoelectron micrograph of a MB found in a hepatoma from a mouse fed GF for 10 months. Note that the reaction product (*arrows*) is localized at the margin of the MB filaments. × 24,100.

This pattern of staining is similar to that reported in both human hepatocellular carcinoma (53–56) and human nodular regenerative hyperplasia (57). A possible explanation for the fact that the cell border stains in hepatomas and hyperplastic nodules was suggested by the electron microscopic observation that the ectoplasm and canaliculi were missing in some tumor cells.

There are some noteworthy parallels between the occurrence of MBs found in man and mice. MBs take months to induce and persist for months after drug withdrawal in both man (58–61) and mice. MBs are seen in benign and malignant hepatic tumors in both man (62, 63) and mice (8, 9). However, the incidence of hepatocellular carcinoma development in human livers which contain MBs is not high in some diseases, i.e., Wilson's disease (64). Therefore, it is premature to draw an analogy between MB formation in man and mice regarding the relationship of MBs to the neoplastic process.

Acknowledgments: Authors wish to thank Dr. B. H. Ruebner for reviewing tumor histology and helpful discussion, Dr. S. Akeda who initiated this work, N. R. Benson for electron microscopical observation and helpful advice, and L. LeFevre and V. Smith for excellent technical assistance. Griseofulvin was generously donated by Schering Corporation, Bloomfield, New Jersey.

REFERENCES

1. Borenfreund E, Bendich A. *In vitro* demonstration of Mallory body formation in liver cells from rats fed diethylnitrosamine. Lab Invest 1978; 38:295–303.
2. Borenfreund E, Higgins PJ, Steinglass M, et al. Carcinogen-induced abnormalities in rat liver cells and their modification by chemical agents. Cancer Res 1979; 39:800–807.
3. Borenfreund E, Higgins PJ, Bendich A. *In vivo-in vitro* rat liver carcinogenesis: Modification in protein synthesis and ultra-structure. Ann NY Acad Sci 1980; 349:357–372.
4. Borenfreund E, Higgins PJ, Peterson E. Intermediate-sized filaments in cultured rat liver tumor cells with Mallory like cytoplasmic abnormalities. J Natl Cancer Inst 1980; 64: 323–333.

5. Borenfreund E, Schmid E, Bendich A, et al. Constitutive aggregates of intermediate-sized filaments of vimentin and cytokeratin type in cultured hepatoma cells and their dispersal by butyrate. Exp Cell Res 1980; 127:215–235.
6. Borenfreund E, Harven ED, Garra L. Mallory body-like abnormalities in carcinoma induced by cultured transformed rat liver cells. Hepatology 1981; 1:408–415.
7. Denk H, Gschnait F, Wolff K. Hepatocellular hyalin (Mallory bodies) in long term griseofulvin-treated mice: a new experimental model for the study of hyalin formation. Lab Invest 1975; 32:773–776.
8. Denk H, Eckerstorfer R, Gschnait F, et al. Experimental induction of hepatocellular hyalin (Mallory bodies) in mice by griseofulvin treatment. 1. Light microscopic observations. Lab Invest 1976; 35:377–382.
9. Meierhenry EF, Ruebner BH, Gershwin ME, et al. Mallory body formation in hepatic nodules of mice ingesting dieldrin. Lab Invest 1981; 44:392–396.
10. French SW, Burbige EJ. Alcoholic hepatitis: clinical, morphologic, pathogenic and therapeutic aspects. In: Popper H, Schaffner F, eds. Progress in liver diseases, Vol VI. New York: Grune and Stratton, 1979:557–579.
11. French SW. Nature, pathogenesis and significance of the Mallory body. Sem Liver Dis 1981; 1:217–231.
12. Fiala S, Fiala AE, Dixon B. Gamma-glutamyl transpeptidase in transplantable chemically induced rat hepatomas and "spontaneous" mouse hepatomas. J Natl Cancer Inst 1972; 48:1393–1401.
13. Kalengayi MMR, Ronchi G, Desmet VJ. Histochemistry of gamma glutamyl transpeptidase in rat liver during aflatoxin B_1-induced carcinogenesis. J Natl Cancer Inst 1975; 55:579–588.
14. Fiala S, Mohindriu A, Ketterling WG, et al. Glutathione and gamma glutamyl transpeptidase in rat liver during chemical carcinogenesis. J Natl Cancer Inst 1976; 57:591–598.
15. Harada M, Okabe K, Shibata K, et al. Histochemical demonstration of increased activity of gamma glutamyl transpeptidase in rat liver during hepatocarcinogenesis. Acta Histochem Cytochem 1976; 9:168–179.
16. Solt DB, Medline A, Farber E. Rapid emergence of carcinogen-induced hyperplastic lesions in a new model for the sequential analysis of liver carcinogenesis. Am J Pathol 1977; 88:595–618.
17. Pitot HC. Stability of events in the natural history of neoplasia. Am J Pathol 1977; 89:703–716.
18. Pugh TD, Goldfarb S. Quantitative histochemical and autoradiographic studies of hepatocarcinogenesis in rats fed 2-acetylaminofluorence followed by phenobarbital. Cancer Res 1978; 38:4450–4457.
19. Cameron R, Kellen J, Kolin A, et al. Gamma glutamyltransferase in putative premalignant liver cell populations during hepatocarcinogenesis. Cancer Res 1978; 38:823–829.
20. Laishes BA, Ogawa K, Roberts E, et al. Gamma-glutamyl transpeptidase: a positive marker for cultured rat liver cells derived from putative premalignant and malignant lesions. J Natl Cancer Inst 1978; 60:1009–1016.
21. Kalengayi MMR, Desmet VJ. Liver cell populations and histochemical patterns of adult and fetal type proteins during Aflatoxin B_1 hepatocarcinogenesis. In: Remmer H, Bolt HM, Bannasch P, et al., eds. Primary liver tumor. Baltimore: University Park Press, 1978: 467–483.
22. Fiala S. Gamma glutamyl transferase during chemical carcinogenesis in rat liver. In: Lehmann FG, ed. Carcinoembrionic proteins, Vol II. Elsevier/North-Holland: Biomedical Press, 1979: 693–698.
23. Huberman E, Montesano R, Drevon C, et al. Gamma-glutamyl transpeptidase and malignant transformation of cultured liver cells. Cancer Res 1979; 39:269–272.
24. Jalanko H, Ruoslahti E. Differential expression of alpha fetoprotein and gamma glutamyl transpeptidase in chemical and spontaneous hepatocarcinogenesis. Cancer Res 1979; 39:3495–3501.
25. San RHC, Simada T, Maslansky CJ, et al. Growth characteristics and enzyme activities in a survey of transformation markers in adult rat liver epithelial-like cell cultures. Cancer Res 1979; 39:4441–4448.
26. Shinozuka H, Sells MA, Katyal SL, et al. Effects of a choline-devoid diet on the emergence of gamma glutamyl transpeptidase-positive foci in the liver of carcinogen-treated rats. Cancer Res 1979; 39:2515–2521.
27. Tsuchida S, Hoshino K, Sato T, et al. Purification of gamma glutamyl transferases from rat hepatomas and hyperplastic hepatic nodules and comparison with the enzyme from rat kidney. Cancer Res 1979; 39:4200–4205.
28. Vanderlaan M, Cutter C, Dolbeare F. Flow microfluorometric identification of liver cells with elevated gamma glutamyl transpeptidase activity after carcinogen exposure. J Histochem Cytochem 1979; 27:114–119.
29. Ogawa K, Solt DB, Farber E. Phenotypic diversity as an early property of putative preneoplastic hepatocyte populations in liver carcinogenesis. Cancer Res 1980; 40:725–733.
30. Lipsky MM, Hinton DE, Klaunig JE, et al. Gamma glutamyl transpeptidase in safrole-induced, presumptive premalignant mouse hepatocytes. Carcinogenesis 1980; 1:151–156.
31. Tamano S, Tsuda H, Tatematsu M, et al. Induction of gamma glutamyl transpeptidase positive foci in rat liver by pyrolysis products of amino acids. Gann 1981; 72:747–753.
32. Enomoto K, Farber E. Kinetics of phenotypic maturation of remodeling of hyperplastic nodules during liver carcinogenesis. Cancer Res 1982; 42:2330–2335.
33. Daoust R. The histochemical demonstration of gamma glutamyl transpeptidase activity in different populations of rat liver cells during azo dye carcinogenesis. J Histochem Cytochem 1982; 30:312–316.
34. Takahashi S, Lombardi B, Shinozuka H. Progression of carcinogen-induced foci of gamma glutamyltranspeptidase-positive hepatocytes to hepatomas in rats fed a choline-deficient diet. Int J Cancer 1982; 29:445–450.
35. Stout DL, Becker FF. Occurrence of progressive DNA damage coincident with the appearance of foci of altered hepatocytes. Carcinogenesis 1982; 3:599–602.
36. Hunt JM, Laishers BA. New hepatocyte phenotypes as early indicators of carcinogenicity. In: Plaa G, Hewitt WR, eds. Toxicology of liver. New York: Raven Press, 1982: 243–290.
37. Rutenberg AM, Kim H, Fishbein JW, et al. Histochemical and ultrastructural demonstration of gamma-glutamyl transpeptidase activity. J Histochem Cytochem 1969; 17:517–526.
38. Nakane PK. Simultaneous localization of multiple tissue antigens using the peroxidase-labelled antibody method: a study on pituitary gland of the rat. J Histochem Cytochem 1968; 16:557–560.
39. French SW, Ihrig TJ, Norum ML. A method of isolation of Mallory bodies in a purified fraction. Lab Invest 1972; 26:240–244.
40. Laemmli UK. Cleavage of structural proteins during the assembly of the head of bacteriophage T4. Nature (Lond) 1970; 227:680–685.
41. Yen S-H, Liem RKH, Jenq L-T, et al. Rapid purification of intact tonofilaments from new born rats. Comparison with glial filaments and neurofilaments. Exp Cell Res 1980; 129:313–320.
42. Sternberger LA. The unlabeled antibody peroxidase-antiperoxidase (PAP) method. In: Sternberger LA, ed. Immunocytochemistry. New York: John Wiley and Sons, 1979: 104–169.
43. Huang S-N, Minassian H, More JD. Application of immunofluorescent staining on paraffin sections improved by trypsin digestion. Lab Invest 1976; 35:383–390.
44. Fuller GM, Brinkley BR, Boughter JM. Immunofluorescence of mitotic spindles by using monospecific antibody against bovine brain tublin. Science 1975; 187:948–950.
45. Kimoff RJ, Huang S-N. Immunocytochemical and immunoelectron microscopic studies on Mallory bodies. Lab Invest 1981; 45:491–503.
46. Irie T, Benson NC, French SW. Relationship of Mallory bodies to the cytoskeleton of hepatocytes in griseofulvin treated mice. Lab Invest 1982; 47:336–345.
47. Bretschneider A, Burns W, Morrison A. "Pop-off" technique. The ultrastructure of paraffin-embedded sections. Am J Clin Path 1981; 76:450–453.
48. Campbell HA, Pitot HC, Potter VR, et al. Application of quantitative stereology to the evaluation of enzyme-altered foci in rat liver. Cancer Res 1982; 42:465–472.
49. French SW, Davies PL. The Mallory body in the pathogenesis of alcoholic liver disease. In: Khanna JM, Israel Y, Kalant H, eds. Alcoholic liver pathology. Toronto: Addiction Research Foundation of Ontario, 1975: 113–143.
50. Denk H, Franke WW, Kerjaschki D, et al. Mallory bodies in experimental animals and man. Int Rev Exp Pathol 1979; 20:77–121.

51. Ohmori T, Rice JM, Williams GM. Histochemical characteristics of spontaneous and chemically induced hepatocellular neoplasms with gamma-glutamyl transpeptidase activity during phenobarbital exposure. Histochem J 1981; 13:85–99.
52. Goldfarb S, Pugh TD, Crippo DJ. Increased alkaline phosphatase activity. A positive histochemical marker for griseofulvin-induced mouse hepatocellular nodules. J Natl Cancer Inst 1980; 64:1427–1433.
53. Takebayashi J, Sagara K, Nagata K, et al. Histo- and bio-chemical observations on gamma-glutamyl transpeptidase in liver diseases. Kumamoto Med J 1972; 25:127–135.
54. Fujisawa K, Kurihara N, Nishikawa H, et al. Carcinoembrionic character of gamma-glutamyltranspeptidase in primary hepatocellular carcinoma. Gastroenterologia Jap 1976; 11:380–386.
55. Gerber MA, Thung SN. Enzyme patterns in human hepatocellular carcinoma. Am J Pathol 1980; 98:395–400.
56. Uchida T, Miyata H, Shikata T. Human hepatocellular carcinoma and putative precancerous disorders. Arch Pathol Lab Med 1981; 105:180–186.
57. Thung SN, Gerber MA. Enzyme pattern and marker antigens in nodular "regenerative" hyperplasia of the liver. Cancer 1981; 47:1796–1799.
58. Horii Y. Electron microscopic studies of livers of drug induced phospholipids. J Kyoto Pref Univ Med 1974; 83:479.
59. Paliard P, Vitrey D, Fournier G, et al. Perhexiline maleate-induced hepatitis. Digestion 1978; 17:419–427.
60. Pessayre D, Bichara M, Feldmann G, et al. Perhexilin maleate-induced cirrhosis. Gastroenterology 1979; 76:170–177.
61. Forbes GB, Rake MO, Taylor DJE, et al. Liver damage due to perhexiline maleate. Clin Pathol 1979; 32:1282–1285.
62. Peters RL. Pathology of hepatocellular carcinoma. In: Okuda K, Peters RL, eds. Hepatocellular carcinoma. New York: John Wiley and Sons Publ., 1976: 107–168.
63. Wetzel WJ, Alexander RW. Focal nodular hyperplasia of the liver with alcoholic hyaline bodies and cytologic atypia. Cancer 1979; 44:1322–1326.
64. Shikata T. Primary liver carcinoma and liver cirrhosis. In: Okuda K, Peters RL, eds. Hepatocellular carcinoma. New York: John Wiley and Sons Publ., 1976: 53–71.